

*Refereed Proceedings*

*The 12th International Conference on*

*Fluidization - New Horizons in Fluidization*

*Engineering*

---

Engineering Conferences International

Year 2007

---

Flow Regime Study in a High Density  
Circulating Fluidized Bed Riser with an  
Abrupt Exit

Joseph Mei\*

Lawrence J. Shadle†

Paul C. Yue‡

Esmail R. Monazam\*\*

\*National Energy Technology Laboratory, Joseph.Mei@NETL.DOE.GOV

†National Energy Technology Laboratory

‡National Energy Technology Laboratory

\*\*REM Engineering Services

This paper is posted at ECI Digital Archives.

[http://dc.engconfintl.org/fluidization\\_xii/6](http://dc.engconfintl.org/fluidization_xii/6)

Mei et al.: Flow regime in High Density CFB

## FLOW REGIME STUDY IN A HIGH DENSITY CIRCULATING FLUIDIZED BED RISER WITH AN ABRUPT EXIT

Joseph S. Mei, Lawrence J. Shadle, Paul C. Yue, Esmail R. Monazam\*,

National Energy Technology Laboratory  
U. S. Department of Energy  
3610 Collins Ferry Road  
Morgantown, West Virginia 26507-0880

\*REM Engineering Services PLLC  
3566 Collins Ferry Road  
Morgantown, West Virginia 26505

### ABSTRACT

Flow regime study was conducted in a 0.3 m diameter, 15.5 m height circulating fluidized bed (CFB) riser with an abrupt exit at the National Energy Technology Laboratory of the U. S. Department of Energy. Local particle velocities were measured at various radial positions and riser heights using an optical fiber probe. On-line measurement of solid circulating rate was continuously recorded by measuring the rotational speed of a twisted spiral vane located in the packed bed region of the standpipe. Glass beads of mean diameter 61  $\mu\text{m}$  and particle density of 2,500  $\text{kg/m}^3$  were used as bed material. The CFB riser was operated at various superficial gas velocities ranging from 3 to 7.6 m/s and solid mass flux from 20 to 550  $\text{kg/m}^2\text{-s}$ . At a constant riser gas velocity, transition from fast fluidization to dense suspension upflow (DSU) regime started at the bottom of the riser with increasing solid flux. Except at comparatively low riser gas velocity and solid flux, the apparent solid holdup at the top exit region was higher than the middle section of the riser. The solid fraction at this top region could be much higher than 7% under high riser gas velocity and solid mass flux. The local particle velocity showed downward flow near the wall at the top of the riser due to its abrupt exit. This abrupt geometry reflected the solids and, therefore, caused solid particles traveling downward along the wall. However, at location below, but near, the top of the riser the local particle velocities were observed flowing upward at the wall. Therefore, DSU was identified in the upper region of the riser with an abrupt exit while the fully developed region, lower in the riser, was still exhibiting core-annular flow structure. Our data were compared with the flow regime boundaries proposed by Kim et al. [1] for distinguishing the dilute pneumatic transport, fast fluidization, and DSU.

### 1. INTRODUCTION

Circulating fluidized bed (CFB) technology has been used commercially in many industries including the power-generation industry [2, 3]. The CFB process has a

number of unique features that make it more attractive than other solid fuel combustion systems in power-generation [4]. Circulating fluidized bed can be operated at different flow regimes, for example, turbulent fluidization, fast fluidization (FF), dilute pneumatic transport (DPT), and dense suspension upflow (DSU). Even though many fluid catalytic cracking (FCC) reactors have been operated at the DSU regime for many years, the DSU flow regime has only recently been identified as being distinct in characteristics from other flow regimes [5]. As pointed out by Grace [5], DSU is distinguished from FF by the higher solids flux ( $>300 \text{ kg/m}^2\text{-s}$ ), higher solids fraction (7-25%), and the absence of particle downflow. During the past decade, many studies were conducted in the fast fluidization flow regime; however, the DSU flow regime has received little attention despite its prominent role in the petroleum industry. Therefore, considerable experimental and theoretical work remains to be done in order to provide a better understanding of this flow regime, which, in turn, will provide a proper basis for the design, scaleup, and operation of reactors operating in the DSU regime. For example, the effects of riser exit and geometry on this regime are still unknowns [5]. The purpose of this study was to investigate this flow regime in an industrial size circulating fluidized bed riser with an abrupt exit. This paper discusses the preliminary data on this flow regime and the effect of a riser with an abrupt exit. Data were also compared with the flow regime boundaries proposed by Kim et al [1] for distinguishing the dilute pneumatic transport, fast fluidization, and DSU.

## 2. EXPERIMENTAL

### 2.1 Apparatus

Figure 1 is a schematic of NETL's cold CFB model. The riser is constructed of flanged steel sections with three 1.22-m acrylic sections installed 2.44, 5.49, and 8.54 m above the solids feed location. Solids enter the riser from a side port 0.23 m in diameter, its centerline 0.27 m above the gas distributor, and exit the riser through a 0.20-m port at  $90^\circ$  about 1.2 m below the top of the riser at a point 15.45 m above the solids entry location (centerline to centerline). Riser velocities were corrected for temperature and pressure as measured at the base of the riser. The mass circulation rate was continuously recorded by measuring the rotational speed of a twisted spiral vane located in the packed bed region of the standpipe. [6] This rate was converted to a mass flux

**Table 1. Glass Beads Characteristics**

|                 |                 |       |
|-----------------|-----------------|-------|
| $\rho_s$        | $\text{kg/m}^3$ | 2426  |
| $\rho_b$        | $\text{kg/m}^3$ | 1384  |
| $d_{sv}$        | $\mu\text{m}$   | 62    |
| $U_t$           | m/s             | 0.225 |
| $U_{mf}$        | m/s             | 0.085 |
| $\epsilon_{mf}$ |                 | 0.421 |
| $\phi$          |                 | 0.86  |

using the measured packed-bed density shown in Table 1, and assuming a constant void fraction at the point of measurement. The solids circulation was varied by controlling the amount of aeration air at the non-mechanical "L-valve" and the standpipe and adjusting the total system inventory to increase standpipe height. Steady-state conditions were defined as holding a constant set of flow conditions and maintaining a constant response in the pressure differentials over a 5-min period. Air velocity and density at the base of the riser was maintained at their desired set-points using both flow control and back pressure control valves. The superficial riser-gas velocity was the sum of the flow at the base of the riser and the aeration air flow at the bottom of the horizontal section of the "L-valve" as well as the other aeration air to the L-valve. Steam was introduced into the air supply header as needed to maintain the relative humidity at approximately 40%.

## 2.2 Measurement method

Mei et al.: Flow regime in High Density CFB

A total of thirty incremental differential pressures were measured across the length of the riser, the standpipe, and the "L-valve" using transmitters calibrated within 0.1% of full-scale or about 2 Pa/m. Twenty of the transmitters were mounted in the riser, eight in the standpipe and two in the "L-valve". The overall riser pressure drop was calibrated within 0.45 Pa/m. Apparent solid fractions were estimated from the measured differential pressures. Particle velocities across the riser at different elevations along the riser were measured using an optical fiber probe. Local particle velocities were measured at different radial positions by traversing the probe horizontally. The probe used was a multi-fiber reflective optical probe developed by Vector Scientific Instruments. The Vector probe contains two 1 millimeter diameter bundles each with 300 minute optical glass fibers. There are equal amounts of randomly distributed transmitting and receiving fibers within each bundle. Light is transmitted through the fibers from a light emitting diode (LED) and the reflected light from the particles is then received by the instrument via photocell. The signal from the photocell is transferred into the computer through an A/D Converter. For each run, 1024 measurements were taken for each of 200 sample periods at a rate of 12.5 kHz over a period of approximately 30 s. The signals from each of the fiber optic bundles were then cross-correlated to determine the particle transit times in each 30 ms sampling periods. The particle velocities were calculated knowing the translational distance between the fibers. The particle velocity was verified using a steel fiber rotated in front of the probe at fixed rates as determined by a stroboscopic sensor. The sampling rate was selected to optimize the probe accuracy over the expected particle velocity range.

## 3. RESULTS AND DISCUSSION

The apparent solids fraction profiles in the riser are displayed in Figure 2 as a function of the solids mass flux ( $G_s$ ) at a given riser gas velocity ( $U_g$ ) of 5.1 m/s. Solids fraction first decreased with increasing height at the lower region ( $h=0-4$  m) and remained fairly constant in the middle region ( $h=4-10$  m) and then, increased with height at the upper region ( $h=10-15.5$  m) of the riser. These apparent solids profiles with an abrupt exit are different than those with a smooth exit, which show solids fraction decreases sharply with increasing height until it reaches the smooth exit [1]. The increase of apparent solids fraction with height in the upper region was attributed to the reflection of solids from the abrupt exit. This abrupt geometry was at a sharp 90 degrees right angle to the vertical upflowing suspension of solid particles. Some of these solid particles could not negotiate the 90 degrees sharp turn and reflected off the top and, therefore, caused solid particles traveling downward along the walls of the riser. As a result, a region of densification was created in the vicinity of the exit of the riser. The extent of the exit effects propagated down the riser depended on the operating conditions and the exit restriction. For Test RPG82 with solid flux  $G_s=125$  kg/m<sup>2</sup>-s at riser gas velocity  $U_g=5.1$  m/s, the abrupt geometry only slightly affected the exit region of the riser. However, as the solids flux increased to  $G_s=283$  kg/m<sup>2</sup>-s, the densification propagated down to about 6.2 m from the exit, exhibiting a more profound exit effect on the riser. The magnitude of the solids fraction decreased from 22.4 % at the top to about 4.5 % at a height of 9.25 m. This was a drop of solid fraction of 2.9 % for each meter. Further increasing  $G_s$  to 424 kg/m<sup>2</sup>-s produced similar apparent solids holdup for both the lower and upper regions. However, for higher solid flux in Test RPG59, the middle region had much higher solids holdup as the dense bed moved upward toward the exit of the riser. The apparent solids fraction in the middle region was greater than 10%. This

suggests that for solid flux,  $G_s = 424 \text{ kg/m}^2\text{-s}$ , and at riser gas velocity,  $U_g = 5.1 \text{ m/s}$ , the entire riser is operating under dense suspension [7]. At higher riser gas velocity,  $U_g = 7.6 \text{ m/s}$  and solid flux, the solids fraction profile, was similar to the profile with lower riser gas velocity,  $U_g = 5.1 \text{ m/s}$  and similar solid flux,  $G_s = 424 \text{ kg/m}^2\text{-s}$ . However, the apparent solids fraction in the middle region decreased to less than 10%. The less solids hold up in the riser may be attributed to the higher solid flux leaving the riser as a result of higher riser gas velocity.

The effect of solids mass flux on the apparent solids fraction in the lower region of the riser at a riser gas velocity,  $U_g = 5.1 \text{ m/s}$ , is shown in Figure 3a. At the lowest two measurement levels, with the differential pressure transmitter at  $h = 0.3 \text{ m}$  and  $h = 0.96 \text{ m}$ , the apparent solids fraction in the bottom of the riser increased with the solids mass flux,  $G_s$ . When  $G_s$  reached about  $280 \text{ kg/m}^2\text{-s}$ , the local solids fraction at the lowest two measurement levels reached constant values of about 0.32 and 0.2 respectively. This suggested that the bottom of the riser was in the dense suspension condition. This dense bed expanded further with a further increase in the solid flux,  $G_s$ , solids mass flux above the  $320 \text{ kg/m}^2\text{-s}$ , to the measurement level of  $h = 3.96 \text{ m}$ , and the solids suspension density increased to 0.18. The apparent solids fraction showed no further increase with increasing solids mass flux. At higher measurement location,  $h = 5.6 \text{ m}$ , which was in the middle section of the riser, solids fraction increased with increasing solids mass flux. At this measurement level, the apparent solids fraction was still developing and had not yet reached its constant level, even though the solids fraction increased to greater than 10% as  $G_s > 380 \text{ kg/m}^2\text{-s}$ . This also suggests that the dense bed was expanding into the middle section of the riser. The effect of solids mass flux on apparent local solids fraction in the upper region near the top exit region of the riser is shown in Figure 3b. According to the criteria of Grace [5] the two locations near the top exit regions were in dense suspension upflow. This was quite different than the data obtained from a smooth exit in which the apparent solids fraction near the top is still in lean phase [1]. This occurrence of dense suspension in the top region, as described previously, was attributed to a sharp, 90 degrees abrupt exit, with large amount of solids being reflected off the top. As a result, a region of densification was created in the vicinity of the exit of the riser. The apparent solids fraction at these two locations,  $h = 14.82 \text{ m}$  and  $13.60 \text{ m}$ , increased with solids flux until it reached  $280 \text{ kg/m}^2\text{-s}$ , then leveled off to a value of 0.23 and 0.14 respectively. The effects of riser gas velocity on the local apparent solids fraction in the lower region near the bottom of the riser is shown in Figure 4. This data was taken at the height of  $0.96 \text{ m}$  measured from the centerline of the horizontal section of the L-valve. At lower gas velocity,  $U_g = 5.1 \text{ m/s}$ , the riser reached the dense suspension at  $G_s = 280 \text{ kg/m}^2\text{-s}$ , as indicated previously, at  $G_s = 280 \text{ kg/m}^2\text{-s}$ . At higher riser gas velocity,  $U_g = 7.6 \text{ m/s}$ , the local apparent solids fraction leveled off to a constant value of about 18% at solid flux,  $G_s = 350 \text{ kg/m}^2\text{-s}$ . This indicated that the riser at that location reached its dense suspension condition. As solid flux increased beyond this value, the apparent local solids fraction remained constant and that the dense bed level expanded as solid flux increased beyond  $350 \text{ kg/m}^2\text{-s}$ . These data also show that at the same solid flux, for example,  $G_s = 400 \text{ kg/m}^2\text{-s}$ , the local apparent solids fraction decreased from 20% to 18% as riser gas velocity increased from  $U_g = 5.1 \text{ m/s}$  to  $7.6 \text{ m/s}$ . The higher solids mass flux required for reaching the dense suspension condition at higher riser gas velocity was expected since a higher gas velocity will carry more solids out of the riser. As a consequence, solids holdup in the riser decreased.

Figure 5 shows the radial particle velocity profiles, measured at five elevations,  $h=0.66, 1.5, 4.5, 8.5,$  and  $13.8$  m along the riser at high gas velocity,  $U_g = 7.6$  m/s, and solid flux,  $G_s = 445$  kg/m<sup>2</sup>-s. At the lowest measurement location,  $h=0.66$  m, particle velocity at and near the wall was very low,  $U_p=0.034$  and  $0.15$  m/s, respectively; however, the solids traveled upward at both locations. At the next measurement level,  $h=1.5$  m, particles at and near the wall, traveled downward, even though the apparent solids fraction was much greater than 7%. The riser at this location, thus, exhibited dense suspension, although it was not a dense suspension upflow (DSU) condition. As the measurement locations moved further up to  $h=4.5$  m,  $8.5$  m, and  $13.8$  m, particles at the riser wall all traveled downward, while the apparent solids fraction at these locations were all greater than 7%. The radial particle velocity profiles measured in the upper region of the riser at the lower riser gas velocity,  $U_g = 5.1$  m/s and  $G_s = 288$  kg/m<sup>2</sup>-s are presented in Figure 6. The local particle velocity, measured at  $h=15.05$  m, showed downward flow near the wall at the top of the riser due to its abrupt exit. This abrupt geometry reflected the solids and, therefore, caused solid particles traveling downward along the wall. However, at the next measuring location,  $h=13.86$  m, the net particle velocities were observed flowing upward at the wall. As data shown previously in Figure 2, for Test RPG88, the apparent solid holdup at the top region of a riser with an abrupt exit was much higher than 7%; therefore, this data in the upper region of the riser could be characterized as DSU regime. However in the lower region of the riser, where the apparent solids fraction was less than 7%, was still exhibiting core-annular flow structure.

Our data is compared with the correlation developed by Kim, et al [1] in Figure 7. The line is the boundary between FF and the DSU regime based on the correlation developed by Kim et al [1]. The solids velocity generated from NETL's data was calculated from the apparent solids fraction along the vertical axis. The regions which have apparent solids fractions less than 7% (as shown in Figure 2, there are only three data points in the middle region of the riser, which are less than 7%) are shown above the red arrow and those greater than 7% are displayed below the red arrow. The riser was operated at dense suspension condition both in the lower and in the upper region. However, based on the particle velocity measurements, particles at and near the wall traveled upward only at the lowest measurement level ( $h=0.66$  m). The rest of the data between the red and blue arrows, therefore, neither belong to the fast fluidization regime nor the DSU regime. Perhaps, a flow regime transition region exists between these two existing flow regimes, where the riser is operated under dense suspension but with net particle velocity at and near the wall still travels downward. The correlation, however, may under predict the apparent solids fraction along the riser. More data are required to confirm this transition from DSU to fast fluidization regime, which may occur both in the lower region and the upper region of a riser with an abrupt exit. The effects of riser geometry and particle properties are not yet well understood for these conditions.

#### 4. CONCLUSION

Flow regime study was conducted in a high density circulating fluidized bed riser of diameter 0.3 m with an abrupt exit. Radial particle velocity profiles were measured using an optical fiber probe at different radial positions by traversing the probe horizontally at various elevations along the vertical axis of the riser. Axial apparent solids fraction profiles were obtained through differential pressure measurements. Under high riser gas velocities and high solid fluxes conditions, a dense region was

created in the vicinity of the exit of the riser due to the reflection of solids from the abrupt exit. Near the top of the riser, a region next to the highest measurement level, particle velocities at and near the wall traveled upward and, as a result, DSU could be reached. Experimental data also supported the notion that transition regions exist in both the upper and lower regions, where dense suspension conditions exist but the net solids flow direction at the wall was still downward. More experiments and analysis are needed to better understand the phenomena leading to dense suspension upflow.

## 5. REFERENCES

1. Kim, S. W., Kirbas, G., Bi, H. T., Lim, C. J., Grace, J. R., 2004, "Flow behavior and regime transition in a high-density circulating fluidized bed riser," *Chemical Engineering Science*, Vol. 59, pp. 3955-3963
2. Berruti, F., Chaouki, J., Godfroy, L., Pugsley, T. S., and Patience, G. S., 1995, "Hydrodynamics of Circulating Fluidized Bed Risers: A Review" *The Canadian Journal of Chemical Engineering*, Vol. 73, pp. 579-602.
3. Reh, L., 1999, "Challenges of circulating fluid-bed reactors in energy and raw materials industries," *Chemical Engineering Sciences*, Vol. 54, pp. 5359-5368.
4. Basu, P., and Fraser, S. A., 1991, "Circulating fluidized bed boilers: design and operations," Butterworth-Heinemann, Stoneham, MA, pp.8-13
5. Grace, J. R., 2000, "Reflections on turbulent fluidization and dense suspension," *Powder Technology*, Vol. 113, pp. 242-248.
6. Ludlow, C., Lawson, L. O. and Shadle, L. J., 2002, "Development of a spiral device for measuring the solids flow in a standpipe," *Circulating Fluidized Bed Technology VII*," J. R. Grace, et al., eds., Canadian Society for Chemical Engineering, Ottawa, Canada, pp. 513-520.
7. Issangya, A. S., Bai, D., Bi, H. T., Lim, K. S., Zhu, J., Grace, J. R., 1999, "Suspension densities in a high-density circulating fluidized bed riser," *Chemical Engineering Science*, Vol. 54, pp. 5451-5460

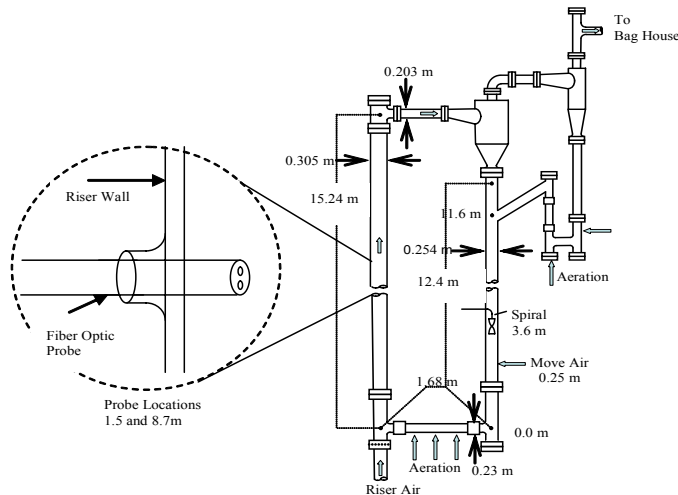


**Figure 1. Schematic diagram of the circulating fluidized bed research facility**

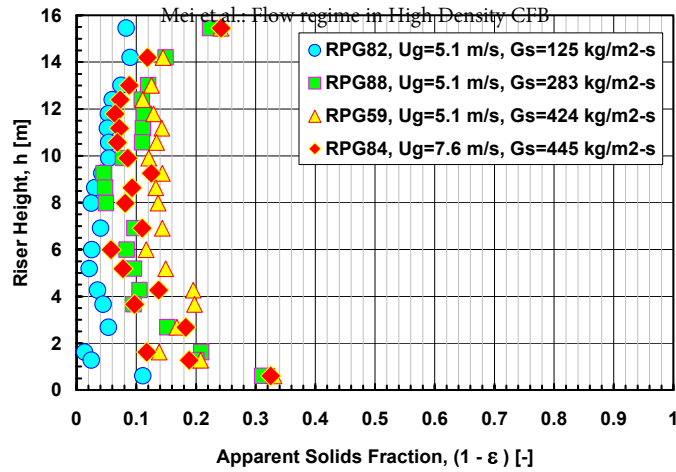


Figure 2. Apparent solids fraction profiles in riser at riser gas velocity,  $U_g = 5.1$  and  $7.6$  m/s and at various solid fluxes

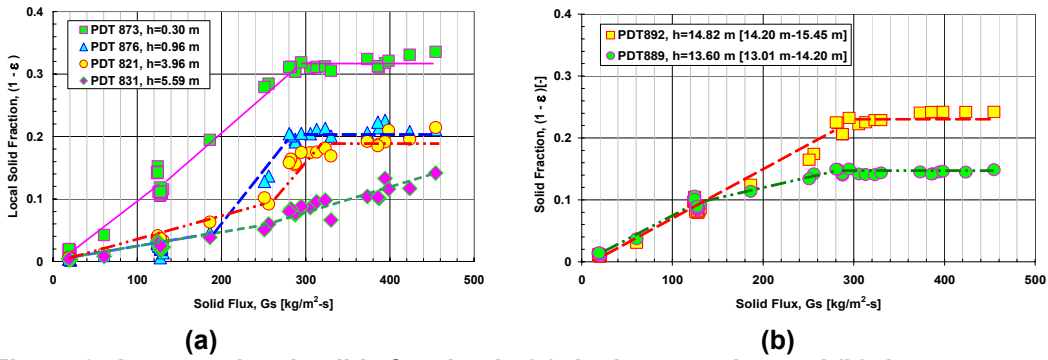


Figure 3. Apparent local solids fraction in (a) the lower region and (b) the upper region of riser as function of solid flux at  $U_g = 5.1$  m/s

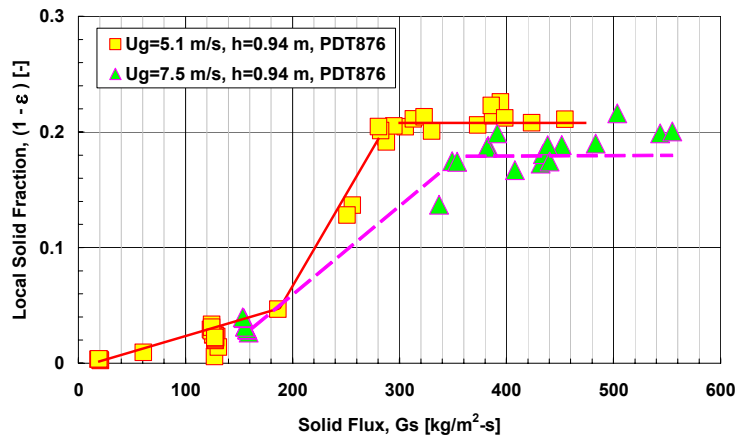


Figure 4. Effect of riser gas velocity on the apparent local solids fraction in the lower region of riser



The 12th International Conference on Fluidization - New Horizons in Fluidization Engineering, Art. 6 [2007]

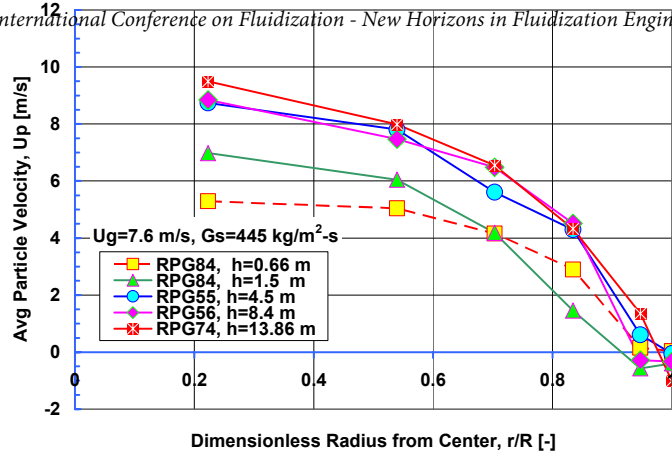


Figure 5. Radial particle velocity profiles in the lower region of riser at  $U_g = 7.6$  m/s and  $G_s = 445$  kg/m<sup>2</sup>-s

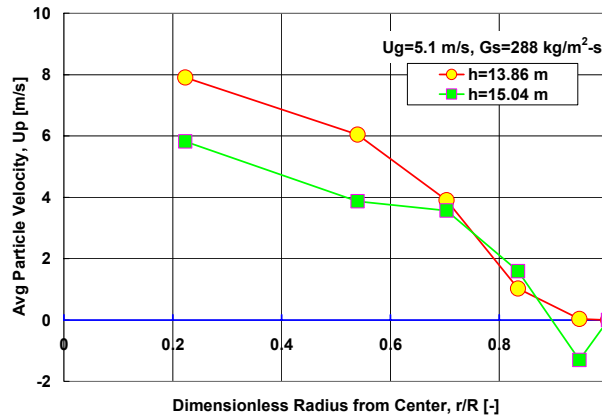


Figure 6. Radial particle velocity profiles in the upper region of riser at  $U_g = 5.1$  m/s and  $G_s = 288$  kg/m<sup>2</sup>-s

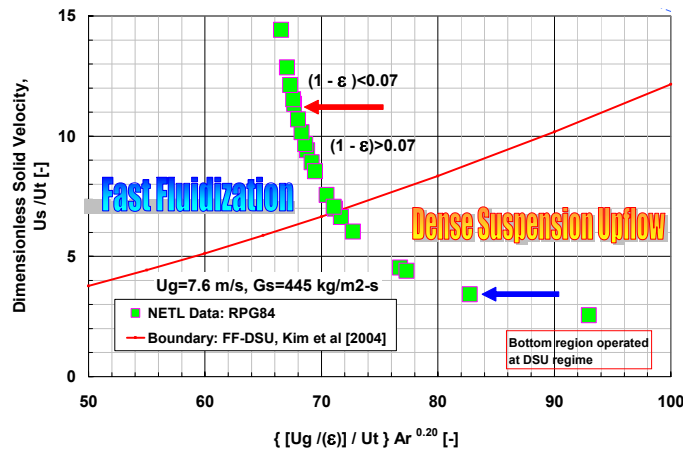


Figure 7. Comparison of NETL data (RPG84,  $U_g = 7.6$  m/s,  $G_s = 445$  kg/m<sup>2</sup>-s) with correlation proposed for boundary between fast fluidization and dense suspension upflow regime by Kim et al [2004].